Journal of Pharmaceutical Sciences 107 (2018) 2119-2127

Contents lists available at ScienceDirect

Journal of Pharmaceutical Sciences

journal homepage: www.jpharmsci.org

Pharmaceutics, Drug Delivery and Pharmaceutical Technology

Superparamagnetic Iron Oxide–Loaded Lipid Nanocarriers Incorporated in Thermosensitive *In Situ* Gel for Magnetic Brain Targeting of Clonazepam

Haidy Abbas [1], Hanan Refai [2,*], Nesrine El Sayed [3]

[1] *Department of Pharmaceutics, Damanhour University, Damanhour, Egypt*
[2] *Department of Pharmaceutics and Industrial Pharmacy, College of Pharmaceutical Sciences and Drug Manufacturing, Misr University for Science and Technology, 6th October City, Egypt*
[3] *Department of Pharmacology and Toxicology, Faculty of Pharmacy, Cairo University, Cairo, Egypt*

ARTICLE INFO

Article history:
Received 27 November 2017
Revised 20 February 2018
Accepted 6 April 2018
Available online 14 April 2018

Keywords:
brain targeting
nanostructured lipid carriers
olfactory route
superparamagnetic iron oxide
thermosensitive *in situ* gel

ABSTRACT

The objective of the study was to target clonazepam to the brain through the intranasal olfactory mucosa using nanolipid carriers loaded with superparamagnetic iron oxide nanoparticles (SPIONs) to allow nanocarrier guidance and retention with an external magnetic field. For improved delivery, the nanolipid carriers were incorporated in a thermosensitive mucoadhesive *in situ* gel. Different nanolipid carriers including solid lipid nanoparticles and nanostructured lipid carriers (NLC) were prepared and characterized with respect to particle size, zeta potential, entrapment efficiency, and *in vitro* release. The NLC composed of 3 solid lipids (Compritol® 888, stearic acid, and glyceryl monostearate) and 2 liquid oils (oleic acid and glyceryl monooleate) showed the most satisfactory characteristics and was loaded with SPION (NLC/SPION). Both formulae (NLC and NLC/SPION) were incorporated in an optimized thermosensitive mucoadhesive *in situ* system composed of 15% pluronic 127 and 0.75% sodium alginate and evaluated for the anticonvulsant action in chemically induced convulsive Swiss Albino mice. The treatment of animals with NLC/SPION significantly prolonged the onset times for convulsion and considerably protected the animals from death. One can thus hope for the emergence of a new intranasal treatment of epilepsy with consequent decrease in peripheral side effects of clonazepam.

Introduction

Epilepsy is one of the most prevalent serious neurological disorders in the world that causes an uncontrolled electrical activity in the brain characterized by seizers. More than 50 million people worldwide suffer from epilepsy, which causes substantial morbidity and mortality.[1] Clonazepam (CZ) is a potent long-acting benzodiazepine derivative that is used mainly for its anticonvulsant, anxiolytic, and amnesic properties by behaving both as a gamma aminobutyric acid receptor agonist and also as a serotonin agonist.[2,3] Benzodiazepines are considered first-line treatments for acute seizures, however they are not recommended for long-term treatment because patients may develop tolerance to their anticonvulsant effects.[4] Current market formulations of CZ release the drug into the peripheral circulation resulting in limited drug uptake across the blood brain barrier (BBB) and in drug distribution to nontargeted sites, which would result in various adverse effects including suicidal thoughts or actions, worsening of depression, sleep disorders, and aggression.[5] Furthermore, orally administered CZ shows extensive first pass metabolism, wide blood level oscillations as well as erratic absorption and bioavailability due to very low water solubility of the drug.[6]

These latter problems, besides the need of a therapeutic prompt action make CZ a good candidate for the development of a brain targeting formulation via olfactory mucosa. Intranasal administration is associated with several advantages including non-invasiveness, ease of application as well as circumvention of the BBB and avoidance of prior absorption to the circulating blood, which minimizes systemic side effects.

CZ has been previously formulated as intranasal delivery systems for olfactory brain targeting for example, mucoadhesive

Abbreviations used: BBB, blood brain barrier; CZ, clonazepam; EE%, entrapment efficiency; Gp I, group I; Gp II, group II; Gp III, group III; i.p., intraperitoneal; Na-alg, sodium alginate; NLC, nanostructured lipid carriers; PF-127, pluronic F-127; PDI, polydispersity index; SLN, solid lipid nanoparticles; SNF, simulated nasal fluid; SPION, superparamagnetic iron oxide nanoparticles; TEM, transmission electron microscopy; $T_{sol/gel}$, gelation temperature.

Conflicts of interest: The authors report no personal financial or non-financial conflicts of interest.

* *Correspondence to:* Hanan Refai (Telephone: 0020106614282).
E-mail addresses: hanan.refai@must.edu.eg, hananrefai71@gmail.com (H. Refai).

https://doi.org/10.1016/j.xphs.2018.04.007
0022-3549/

microemulsion,[7] microspheres,[8] polymeric micelles,[9] and transfersomes.[10] It has been also formulated as solid lipid nanoparticles (SLN) for oral and parenteral administration.[11] To our knowledge, CZ has not been formulated as SLN and nanostructured lipid carriers (NLC) for intranasal administration.

Nanolipid carriers have received increasing attention in the last several years for their physicochemical stability, biocompatibility, and capability of controlled drug release. In addition, they have good tolerability and biodegradability, lack of acute and chronic toxicity of the carrier, and scalability. Furthermore, nanolipid carriers by virtue of their lipophilic nature and very small particle size enhance greatly the brain uptake of many drugs.[12,13] However, nasal mucociliary clearance is one of the most important limiting factors for nasal drug delivery.[14] To overcome this problem, an increase in the contact time between dosage form and mucosal layers of nasal cavities is required, thus enhancing drug uptake as well as preventing rapid nasal clearance mucosal surface. *In situ* gelling systems are viscous liquids, which are transformed into a gel, when applied to human body, due to change in temperature, pH, or ionic strength.[15] Unlike preformed gels, they allow accurate and reproducible administration of a drug and could prolong the formulation's residence time to the mucosal surface due to post-administration gelling.[16]

For improved drug targeting, drug carrier with enclosed magnetic nanoparticles could be guided with the help of an external magnetic field to the target tissue.[17] Superparamagnetic iron oxide nanoparticles (SPION) are small synthetic γ-Fe_2O_3 (maghemite), Fe_3O_4 (magnetite), or α-Fe_2O_3 (hematite) particles with a core ranging from 10 to 100 nm in diameter. In addition, due to the essential characteristics, SPIONs exhibit unique electronic, optical, and magnetic properties that have been widely used in *in vivo* biomedical applications.[18]

Accordingly, the main objective of the present study was to develop CZ-loaded nanolipid carriers as brain-targeting delivery system via the olfactory mucosa with the aim of enhancing the brain uptake of the drug, to attain rapid onset of action with good efficacy at lower doses. The nanolipid carriers were formulated in a mucoadhesive thermosensitive *in situ* gelling system to prolong the residence time of the formulation at site of administration. Furthermore, for improved targeting as well as increased retention time SPIONs were encapsulated into the lipid matrix where the nanolipid carriers could be directed to the target tissue by applying an external magnetic field.

Materials and Methods

Materials

CZ was kindly supplied from Egyptian International Pharmaceutical Industries Company (Tenth of Ramadan City, Egypt). Poloxamer 407 (Pluronic F-127) was obtained from BASF (Ludwigshafen, Germany). Pentylenetetrazole was obtained from Sigma-Aldrich (Steinheim, Germany). Oleic acid, tween 80, stearic acid, and sodium alginate (Na-alg) were purchased from Elgomhoreya, Egypt. Glycerol monostearate, glyceryl monooleate, and glyceryl behenate (Compritol® 888) were kindly supplied from Gattefossé (Saint-Priest, France). All other reagents were of analytical grade.

Methods

Preparation of SLN and NLC

CZ-loaded SLN and NLC were prepared by high-pressure homogenization technique. Table 1 provides the composition of all developed nanolipid carriers. SLN formulations contained only solid lipids, whereas in NLC formulations, 15% of the solid lipids were replaced by oil (glycerol oleate and oleic acid). The total lipid phase was kept constant (1%) in all formulations. The lipid components were blended and melted at 70°C until a clear oil phase was obtained. The aqueous phase containing 2% tween 80 was heated to the same temperature as the lipid phase. The hot aqueous phase was added to the melted lipid phase and directly homogenized using high pressure homogenizer at 75°C and 500 bar (Wiggen Hauser, Berlin, Germany) at 18,000 rpm for 5 min followed by 10 min homogenization at 22,000 rpm. The obtained emulsion was then homogenized at 25,000 rpm for 5 min. The homogenization rate decreased gradually from 25,000 to 22,000 rpm then to 18,000 rpm each for 2 min. For the preparation of SPION-loaded NLC, 0.7 mL of aqueous dispersion of SPION (10.3 mg/mL) was added and sonicated using a probe sonicator (Branson Sonifier®) for 10 s. The coarse emulsion was then subjected to probe sonication for 1.5 min at 50% amplitude and a power of 100 W. To prevent temperature increase, the probe sonicator was inactive in 2-second intervals. The emulsion was then cooled down in an ice bath for 30 min to recrystallize the lipids and form SLN or NLC. The formulae were freeze-dried at −80°C and 0.001 mbar for 48 h (Martin Christ, Alpha 1-2 LD; Vacuubrand GMBH + Co KG, Wertheim, Germany) and stored at 4°C.

Preparation of SPION

Ferric chloride hexahydrate (1.17 g) and ferrous sulphate tetrahydrate (0.6 g) in a molar ratio of 1.75:1, respectively were dissolved in 50 mL of deionized water and stirred vigorously under N_2 atmosphere at 70°C. After 1 h, 5 mL of ammonium hydroxide (32%) was rapidly injected into the mixture and stirred for another 1 h and then cooled to room temperature. The black precipitate (magnetite, Fe_3O_4) was separated by magnet, and the particles were washed 5 times with hot water and dried in an oven at 50°C overnight.

Characterization of CZ Nanolipid Carriers

Particle Size, Polydispersity Index, and Zeta Potential. The mean particle size, size distribution, and zeta potential of freshly prepared SLN and NLC were assessed using a Malvern Zetasizer 2000 (Malvern Instruments Ltd., Malvern, UK). The measurements were performed after diluting samples by 100-fold with water at ambient temperature.

Table 1
Composition of CZ, NLC, and SLN

Formula	Composition (mg)				
	Glycerol Monostearate	Stearic Acid	Compritol	Oleic Acid	Glycerol Oleate
F1	850		150		
F2		850	150		
F3	700		150	75	75
F4		700	150	75	75
F5	350	350	150	75	75

Entrapment Efficiency. The amount of drug entrapped in the nanolipid carriers was determined by calculating the difference between the total amount of CZ used to prepare the nanocarriers and the amount of nonentrapped drug remaining dissolved in the aqueous dispersion medium. One milliliter of CZ-loaded SLN or NLC dispersion was centrifuged at 10,000 rpm and 4°C for 10 min (cooling ultracentrifuge 3-30 K; Sigma-Aldrich) to separate the drug-loaded nanolipid carriers from the supernatant containing unloaded CZ. The supernatant was analyzed for the free drug spectrophotometerically at 254 nm (UV spectrophotometer; Shimadzu). The drug entrapment efficiency (EE%) of nanocarriers was calculated as indicated in the following equation.[19]

$$EE\% = \frac{A - B}{A} \times 100$$

where A is the total amount of drug in the nanocarrier and B is the free amount of drug in the supernatant.

In Vitro *Drug Release.* The release of CZ from SLN and NLC formulations was evaluated using the dialysis technique. Two grams of each formulation (equivalent to 1 mg of CZ) were placed in a dialysis bag (Spectra/Por® membrane MWCO 100,000 Spectrum), then sealed at both ends with medicell clips (Spectrum) and attached to the paddle shafts of a USP dissolution apparatus (Pharma Test, Hainburg, Germany), and suspended in 250 mL phosphate buffer pH 6.5. The study was carried out at 36 ± 0.5°C using an agitation speed of 50 rpm. Aliquots of 2 mL were withdrawn from the dissolution medium at regular time intervals and replaced by fresh phosphate buffer. The drug concentration was determined spectrophotometrically at 254 nm. Blank experiment using plain nanocarrier dispersions was carried out at the same conditions. The experiment was performed in triplicate. Kinetic analysis was subsequently carried out according to zero and first orders and Higuchi[20] diffusion model. The model with the highest coefficient of determination was considered the best fitting.

Morphology of Nanocarriers. Surface morphology of NLC and NLC/SPION was studied by transmission electron microscopy (TEM; JEOL JEM-1230, Tokyo, Japan). One drop of each formula was loaded onto a copper grid. The formulae were stained with 1 drop of phosphotungstic acid aqueous solution (2% w/v) for 3 min prior examination.

Preparation of Plain Mucoadhesive In Situ *Gel*

For intranasal application, thermosensitive pluronic F-127 (PF-127)–based *in situ* gels containing Na-alg as anionic mucoadhesive polymer were formulated. Na-alg was dissolved first in water, and then PF-127 was dispersed in cold Na-alg solution with continuous magnetic stirring. The dispersion was kept in refrigerator (4°C) for at least 24 h to ensure complete dissolution. Cold distilled water was then added to complete the volume. The composition of the tested *in situ* gel formulations is shown in Table 2.

Preparation of In Situ *Gels Incorporated With CZ Nanolipid Dispersion*

In situ gel base with optimum characteristics was used for the incorporation of the nanolipid dispersion that revealed satisfactory particle size, EE% and drug release. The nanolipid dispersion was embedded into equal volume of plain *in situ* gel at 4°C, by magnetic stirring until the formation of a homogenous preparation.

Evaluation of the Prepared In Situ *Gels*

Physical Appearance. All formulations were visually inspected for general appearance, color, and clarity before and after gelling.

Determination of pH. A calibrated pH meter (Elico, Hyderabad, India) was used to determine the pH of the formulations. The measurement was carried out in triplicate.

Determination of Gelation Time. It was carried out according to the tube inversion method reported by Asasutjarit et al.[21] Briefly, 2 mL of the *in situ* gel were put in a test tube and kept at 4°C for 2 h, then placed in a water bath adjusted at the gelation temperature (37°C). The *in situ* gel was observed for gelation by inverting the test tube at periodic intervals. The gelation time was detected when the liquid meniscus would no longer move upon tilting the test tube through an angle of 90°.

Determination of Gelation Temperature ($T_{sol/Gel}$). Fixed weight (10 g) of each sample was placed in a glass vial containing a magnetic bar (15 mm × 6 mm). The formulations were heated starting from 20°C by constant rate (1°C/min) while being stirred at 100 rpm. The $T_{sol/Gel}$ was recorded when the magnetic bar stopped moving.[22] The evaluation was repeated 3 times for each formulation.

Bioadhesive Strength. It was measured according to a method reported by Sultana et al.[23] using a modified physical balance, the right pan of which was replaced by a glass plate (4 × 4 cm). A section of freshly dissected rabbit nasal mucosa was glued to the lower side of the glass plate with α-cyanoacrylate glue. The gel was spread over 1 cm^2 on another piece of mucosa, which was adhered to a moving platform. The platform was slowly raised until the gel touched the upper mucosa. The mucosal surfaces were held in contact for 2 min then weights were put onto the left pan until membranes got detached.[24] The minimum weight required to detach the membranes was recorded ,and the bioadhesive force expressed as the detachment stress in dynes/cm^2 was calculated using the following equation[25]:

$$\text{Mucoadhesive strength}\left(\text{dyne.cm}^2\right) = \text{m.g/A}$$

where, m is the weight required for detachment (g), A is the area of mucosa exposed (cm^2), g is the acceleration due to gravity (980 cm/s^2). The experiment was performed in triplicate.

Table 2
Composition and Characterization of Different *In Situ* Gelling Formulations

Formula	PF-127 (% w/w)	Na-alg (% w/w)	$T_{sol-gel}$ (°C)	Gelation Time (s)	pH	Viscosity (cp)			Mucoadhesive Force (dyne/cm^2)
						4°C	37°C	37°C/SNF	
G1	15	0.25	>40	40 ± 1.8	5.5 ± 0.1	68 ± 5.5	852 ± 10.6	901 ± 6.4	71.5 ± 2.6
G2	15	0.50	35.1 ± 0.6	33 ± 1.9	5.5 ± 0.3	83 ± 4.7	1226 ± 8.2	1300 ± 7.7	81.0 ± 2.2
G3	15	0.75	32.8 ± 0.6	31 ± 2.1	5.6 ± 0.6	89 ± 6.1	1456 ± 7.7	1524 ± 9.4	100.3 ± 2.8
G4	17	0.25	28.1 ± 0.3	27 ± 1.4	5.6 ± 0.3	74 ± 6.1	923 ± 9.2	1114 ± 5.9	68.0 ± 4.2
G5	17	0.50	27.2 ± 0.6	26 ± 1.1	5.9 ± 0.4	87 ± 4.2	1233 ± 7.1	1384 ± 9.7	84.2 ± 3.6
G6	17	0.75	22.6 ± 0.3	25 ± 2.1	6.2 ± 0.4	91 ± 5.9	1501 ± 7.9	1587 ± 8.3	103.0 ± 2.9

Determination of Viscosity and Rheological Behavior. The viscosity measurement was determined using a cone and plate viscometer (Brookfield programmable DVII + Model pro II type). To study the effect of temperature on the viscosity of the *in situ* gels, the spindle was rotated at constant speed (10 rpm), and the apparent viscosity was measured at both 4°C and 37°C. The viscosity was also determined in the presence of simulated nasal fluid (SNF). SNF was prepared by dissolving 0.745 g of sodium chloride, 0.129 g of potassium chloride, and 0.005 g of dehydrated calcium chloride in 100 mL distilled water. To study the rheological behavior, the prepared solutions were allowed to gel at 37°C, and then viscosity was measured at different angular velocities (10, 20, 30, 40, and 50 rpm) with 10 s between each 2 successive speeds and then was repeated in a descending order of velocity.

Anticonvulsant Action Evaluation. The anticonvulsant action of *in situ* gel incorporated with CZ-loaded NLC and NLC/SPION was studied on chemically induced convulsions in Swiss Albino mice.

Animal Housing and Handling. The protocol for the study was approved by the Institutional Animal Ethics Committee of Faculty of Pharmacy, Cairo University, Egypt, and they comply with the ARRIVE guidelines. Swiss Albino mice (22-25 g body weight) provided from the animal house of the national research center, Cairo, Egypt were housed in plastic cages and kept in a conditioned atmosphere at 22 ± 3°C and humidity 50%-55% with 12 h light/dark cycles for at least 1 week for stabilization. They were fed standard pellet chow (El-Nasr Chemical Company, Cairo, Egypt) and were allowed free access to water.

Chemical Induction of Convulsions. Mice were divided into 3 groups of 10 animals each. Group I (Gp I) and group II (Gp II) received *in situ* gel incorporated with CZ-NLC and CZ-NLC/SPION, respectively, and group III (Gp III), the control group, received no medication. Each animal of Gp I and Gp II was anesthetized with ketamine (60 mg/kg) by intraperitoneal administration (i.p.), and then, a volume of 10 μL of different formulae containing 0.04-0.05 mg CZ (equivalent to 0.2 mg/kg body weight) was administered in each nostril. Formulations were instilled deeply into the nostrils with the help of (2-20 μL) high-performance micropipette to which tips of 0.1 mm in diameter were fixed. Rats of Gp II were placed supinely on a platform with their heads positioned directly on a neodymium–iron–boron magnet. Each animal was then allowed to rest for fixed time (5 min) to recover completely from the anesthesia and to allow time for the drug to reach the brain. Five minutes after the administration of formulae, clonic convulsions were induced in mice by pentylenetetrazole (100 μg/kg, i.p.)[26]; then animals were immediately placed under an acrylic glass box and observed for 30 min both visually and via a video camera. For comparison, the control group (GP III) sham-treated with no drug administered was injected (i.p.) with pentylenetetrazole at a dose of 100 mg/kg. For each animal, the onset time of the first clonic convulsion and time of death were recorded.

Statistical Analysis. Results were statistically analyzed using automated software (Prism Software version 5.01; Graph Pad Inc., San Diego, CA). Results were reported as mean ± standard error. Significant differences between the control and treated groups were calculated using nonpaired "t" test, and $p \leq 0.05$ was taken as significant.

Results and Discussion

Evaluation of CZ-Loaded SLN and NLC

CZ-loaded SLP and NLC were prepared by hot homogenization technique method using different types of solid and liquid lipids and different drug to lipid ratios. The formulations were evaluated for particle size, zeta potential, EE%, and *in vitro* release to select the optimum formulation to be incorporated into *in situ* nasal gel.

Particle Size, Zeta Potential, and EE%

Solid lipid, oil as well as surfactant type and concentration play a crucial role in deciding the size, charge, and drug entrapment. The mean particle size, polydispersity index (PDI), zeta potential, and EE % of the different formulae are shown in Table 3.

Entrapment Efficiency. Loading capacity of the drug in lipid nanocarriers is mainly controlled and dependent on the solubility of the drug in the lipid melt. The lipophilic nature of CZ with a partition coefficient of log *p* (octanol/water) = 2.41 favors its residence in lipid carriers, which consequently increases the drug loading.[27] Moreover, Compritol 888 probably increases drug entrapment due to the presence of large amounts of mono-, di-, and tri-glycerides that help in drug solubilization. Also, the less-defined mixture of acylglycerol provides additional space for entrapping drug molecules. From Table 3, it is noticed that the EE% of all NLC formulations (F3, F4, and F5) showed significantly ($p < 0.05$) higher values in comparison to SLN (F1 and F2). This is probably because of the transformation of solid lipids during the cooling process to more ideal crystal state of higher order and lower energy modification, which increases the tendency of solid lipids toward attaining structural perfection that leaves hardly any space to lodge drug molecules. Consequently, this result in drug expulsion and poor drug payload.[28] This phenomenon is even more pronounced when pure lipids are used. Because of this reason, 2 different solid lipids, glycerol monostearate (GMS) or stearic acid (SA) and compritol, were incorporated. Applying liquid lipid in the mixture led to limitation of recrystallization and the formation of amorphous or less ordered crystalline state, which resulted in imperfection and accommodation of higher amount for encapsulant. The highest state of imperfection is thus expected to be in F5 that is composed of 3 different solid lipids in addition to 2 liquid lipids, and this formulation in deed showed the highest entrapment. Furthermore, higher EE% in NLC could be also due to the higher solubility of the drug in liquid oil than solid lipids.[29]

Table 3
Physicochemical Properties of CZ, NLC and SLN, and SPION

Formula	Particle Size (nm)	Zeta Potential (mV)	EE (%)	PDI	Drug Released (%)
F1	272.6 ± 21.84	−25.6 ± 0.58	52.6 ± 1.35	0.369 ± 0.06	79.2 ± 0.84
F2	277.1 ± 18.52	−27.1 ± 0.78	49.2 ± 1.55	0.199 ± 0.04	70.4 ± 0.96
F3	288.8 ± 34.21	−32.4 ± 0.51	59.3 ± 1.68	0.237 ± 0.03	64.3 ± 2.63
F4	220.1 ± 32.85	−28.9 ± 0.26	61.4 ± 1.74	0.206 ± 0.07	86.9 ± 2.12
F5	210.2 ± 12.67	−34.1 ± 0.21	65.7 ± 1.81	0.197 ± 0.08	94.1 ± 1.18
F5S	209.6 ± 7.35	−25.2 ± 2.96	ND	0.166 ± 0.05	ND
SPION	10.2 ± 1.2	21.3 ± 0.34	–	0.142 ± 0.02	–

ND, not determined.

Zeta Potential. Zeta potential can be considered as an important indicator of physical stability of nanodispersions. A higher electric charge on the surface of the nanoparticles will prevent aggregation because of the strong repellent forces among particles giving more stable dispersions.[30] The results listed in Table 3 show that all formulae possess negative surface charge and absolute zeta potential values above 20 mV, which indicates that nanosuspensions are well dispersed with considerable stability.[31] Most of the lipids included in the lipid nanocarriers being glycerol esters of long-chain length fatty acids would probably provide neither charge nor polarity that contributes to zeta potential. However, because of the nonesterified hydroxyl groups of the glycerol and the length of the fatty acids, the molecule exhibits certain polarity that contributes to zeta potential, which explains the relatively high zeta potential values. Moreover, the surfactant used in the formulation, despite being nonionic, may polarize and adsorb polarized water molecules at the surface of particles.[32] On the other hand, the fatty acids, that is, oleic acid and stearic acid contribute to the negative charge on the lipid carriers. The formulations that contained stearic acid (F2, F4, and F5) shifted the zeta potential to higher negative values. Noticeably, the formulation F5, which contained lower content of stearic acid, had higher zeta potential value. A similar finding was observed by López-García and Ganem-Rondero,[33] who suggest that it might be because of the accumulation of oil at the surface of NLC. When preparing NLC, the solid lipid recrystallizes first, because the melting point of the solid lipid is higher than that of the oil, holding a portion of the oil within the solid lipid matrix. Subsequently, the excess of oil remains in the outer shell of nanolipid carriers, thus contributes to zeta potential. The oil phase in the present NLC systems includes oleic acid, which carry a negative charge thus a shift would occur to higher negative values.[34] The reason why this effect was more pronounced in the case of F5 in comparison to other NLC systems (F3 and F4) might be based on the increased imperfection in the crystalline state, which probably led to increased oil on the surface of the particles.

PDI and Particle Size. From the results, it was observed that all formulated lipid nanocarriers had PDI values lower than 0.5 indicating their narrow size distribution. Regarding the particle size, it was expected that NLC formulae would all show smaller sizes than SLN formulae based on a study conducted by Kelidari et al.,[35] who reported that the addition of oils reduces the viscosity of the NLC suspensions, which subsequently decreases the surface tension and the particle size. Furthermore, Puglia et al.[6] stated that the addition of liquid oil increases the molecular mobility of the matrix, which leads to the formation of smaller particles. However, these postulations could not be applied to all formulations in the present study. The NLC formulae that contained stearic acid in addition to the liquid oil phase (F4 and F5) showed significantly smaller sizes (p <0.05) than the NLC formula containing GMS (F3), which has a particle size in the same range as SLN formulae. This is probably attributed on one hand to higher molecular weight and consequently higher viscosity of GMS in comparison to stearic acid and on the other hand to increased surface coverage of stearic acid in the case of NLC particles as previously explained. Because of good emulsifying properties of stearic acid, this could reduce the surface tension and hence the particle size.

In Vitro *Drug Release*

Kinetic analysis of *in vitro* release data revealed that the release profiles of all SLN and NLC formulae followed square root time dependent Higuchi model, which is described as a diffusion process based on Fick's law. As illustrated in Figure 1, the release pattern of the formulations was biphasic with an initial fast release for the first 30 min followed by a more gradual sustained release. The

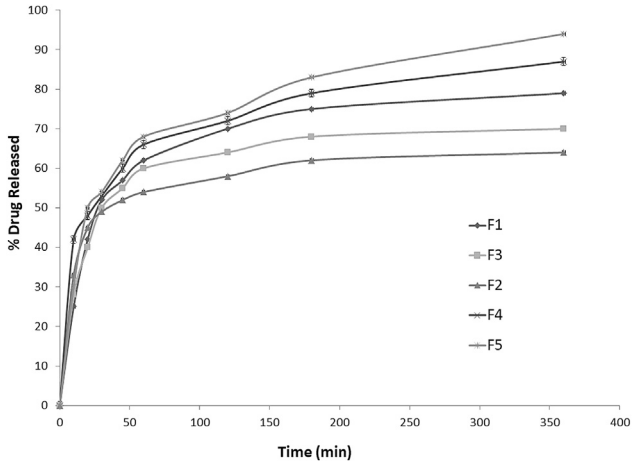

Figure 1. Percent release of CZ from different nanolipid carriers (n = 3).

initial burst of CZ was probably because of the free drug present in the formulations, which was not entrapped in the nanolipid carriers, in addition to the amount of drug attached to the surface of particles,[36] whereas the second phase is probably due to slow diffusion of the drug from the nanoparticles.

The results show a significant higher release for F2 in comparison to F1. The difference between the 2 SLN formulations is based on the type of solid lipid other than compritol. It is believed that in case of F1, the SLN acquire a shell/core configuration similar to that suggested by Souto et al.[37] This belief relies on the difference in melting point between GMS (58-59 C) and compritol (69-4 C). Owing to higher melting point, upon cooling compritol probably solidifies first forming a shell that encloses a core of GMC. Aburahma and Badr-Eldin[38] reported that Compritol 888 ATO has a more pronounced hydrophobic property compared to esters of glycerin with either palmitic (C16) or stearic acid (C18), attributed to longer fatty acid chain length in behenic acid (C22). Because of increased lipophilicity of the drug,[27] the drug probably concentrates more in the outer shell composed of compritol, which explains the higher release rate of the drug from F1. On the other hand, because the melting point of stearic acid (69.3 C) is close to that of compritol, both lipids would solidify together forming a matrix type particle, which would result in increased existence of stearic acid with lower drug content at the surface of the particles. This is in accordance with the higher negative value of zeta potential observed for this formula. Consistent with these results, a study conducted by Priyanka and Sathali,[39] which investigated SLN composed of different solid lipids, showed that, the drug loading was in the order of compritol > GMS > stearic acid. The results are also in accordance with the hydrophilic lipophilic balance (HLB) values of the lipids, which are 2, 3.8, and 15 for compritol, GMS, and stearic acid, respectively, which indicate that a highly lipophilic drug like CZ would concentrate more in a lipid with lower HLB value.

However, the case was totally reversed when liquid lipids were introduced. Comparing the SLN and NLC formulae containing GMS (F1 and F3, respectively), the existence of oil phase reduced the rate of drug release significantly. Nevertheless, in the case of SLN and NLC formulae containing stearic acid (F2 and F4, respectively), an obvious increase in drug release was observed, when oils were added. This is probably related to the emulsifying properties of the lipids. Because of higher HLB value of stearic acid, the oil is distributed more to the outer surface, which leads to the formation of drug-enriched oily regions at the surroundings and consequently enhanced the drug release,[40] while in the case of GMS which has a low HLB value that is close to compritol, the oil is probably more

homogeneously distributed within the matrix. This is in accordance with Swidan et al.,[29] who stated that, slow release profile of drug from NLC is due to homogeneous entrapment of the drug throughout the system.

Selection of Optimized Formula and Evaluation of SPION-Loaded NLC

Based on the physical characterization of the SLN and NLC formulae, F5 was selected for the incorporation of SPION (F5S) and for further studies as it showed the smallest particle size, highest EE %, and drug release as well as the greatest absolute zeta potential value. The incorporation of SPION, which was found to be in the size of 10.2 ± 1.2 nm, did not significantly affect the NLC particle size, but it resulted in an obvious reduction in zeta potential absolute value. This is probably due to the attachment of the positively charged iron oxide nanoparticles (Table 3) to the surface of the NLC particles, which could have decreased the negativity of the particles to some extent.

Transmission Electron Microscopy

Morphologic examination was carried out on the selected optimum NLC formula (F5) and NLC/SPION (F5S). As shown in Figure 2, the lipid nanoparticles were distinct, spherical with smooth surface, which would probably facilitate the drug targeting into internal tissues of the olfactory nerve.[41] The NLC particles (F5) seemed to have an outer shell, which is probably an indication to higher concentration of oil phase on the periphery. This is consistent with the increased drug release and higher zeta potential value observed for this formula. Furthermore, the nanoparticles appeared to be considerably smaller than the average particle size that was determined by the zetasizer. This may be attributed to the hydrodynamic layers that form around the particles leading to an overestimation of the particles' size when determined by zetasizer.[42] This also supports the belief of the presence of higher concentration of surfactants at the surface that holds the oil phase at particles' periphery. NLC/SPION particles had similar morphologic features to NLC particles, but they were obviously larger in size probably due to incorporation of iron oxide nanoparticles. However, this size difference could not be observed in zetasizer measurements. The enclosure of SPION probably changed the surface characteristics of NLC/SPION particles and decreased the adhered hydrodynamic layers. This would make them appear smaller in zetasizer measurements than they actually are. Moreover, NLC/SPION particles did not seem to have a distinct outer shell like that of NLC particles, which may further indicate different phase arrangement.

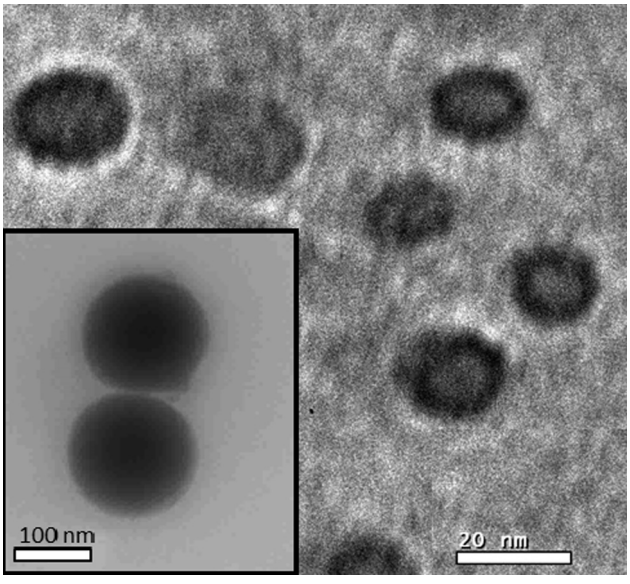

Figure 2. TEM photomicrograph of NLC particles (F5). The inset shows the TEM image of NLC/SPION particles (F5S).

Evaluation of In Situ *Gelling Systems*

For intranasal administration of CZ, an intranasal formulation was developed based on a nanotechnology *in situ* gelling strategy, which can improve mucous membrane permeability, avoid runoff from the nasal cavity, and to retain the drug at the absorption site for an extended duration. To modulate the *in situ* gel properties and select accordingly the most suitable formulation to incorporate the optimized NLC formula, *in situ* gel systems were prepared with 2 different concentrations of PF-127 (15% and 17%) and mixed with different concentrations of Na-alg (0.25%, 0.5% and 0.75%). Na-alg was added for its ion sensitive *in situ* gelling property, when it comes in contact with Ca^{2+} ions present in the nasal fluid in addition to improving mucoadhesion, enhancing viscosity, and extending drug release of PF-127 gel under physiological conditions.[43] The *in situ* gel systems were evaluated for gelation temperature, gelation time, pH, viscosity, and mucoadhesive strength (Table 2).

Physical Appearance and pH

All gels were glassy clear in appearance. Gel pH was in the range of 5.5-6.2, which is suitable for intranasal administration. Arora et al.[44] reported that the pH of the nasal formulation should be adjusted to 4.5-6.5 to avoid nasal irritation, obtain efficient drug permeation and prevent the growth of bacteria.

Gelation Temperature

Gelation temperature is the temperature at which the liquid transfers to a transparent gel and is considered a very important parameter for assessing *in situ* gelling preparations. Liquids having $T_{sol\text{-}gel}$ of ~28°C-37°C are considered suitable for nasal application.[45] *In situ* gelling systems with $T_{sol\text{-}gel} \leq 28°C$ may transform to gel at room temperature.[46] From Table 2, it is to be noticed that G1 had a $T_{sol\text{-}gel} > 40°C$, and the formulae G4 to G7 gelled at temperatures ≤28°C being therefore unsuitable for *in situ* gelling, whereas the formulae G2, G3, and G4 showed acceptable gelation temperatures in the range of 32°C-35°C. It was observed that, the increase in the concentration of PF-127 from 15% (G1-G3) to 17% (G4-G7) was accompanied by a decrease in the gelation temperature (Table 2). PF-127 is an amphiphilic synthetic copolymer consisting of 2 hydrophilic polyethylene oxide (PEO) blocks and a hydrophobic polypropylene oxide (PPO) block. These amphiphilic molecules assemble in aqueous solutions and form large micellar cross-linked network when their concentration exceeds the critical micelle concentration.[47] Micelle formation is not only concentration dependent but it is also greatly influenced by temperature. At lower temperatures, both PPO and PEO blocks are hydrated. When temperature increases, the PPO chains become dehydrated and less soluble than the PEO chains. This results in hydrophobic interactions among the PPOs and the formation of spherical micelles with a dehydrated PPO core and an outer hydrous PEO shell. Such micelles entangle with other micelles and form a 3-dimensional network structure.[48] Therefore, at lower concentrations of PF-127, higher temperatures are needed for gelation. As the concentration of PF-127 increases, the gel structure becomes more closely packed with the arrangement in the lattice pattern, and gelling occurs rapidly at lower temperature.[49]

Also, the presence of Na-alg lowered the gelation temperature. This could be explained by the ability of Na-alg to bind to the polyoxyethylene chains present in the pluronic molecules through hydrogen bonds which promotes dehydration causing an increase in entanglement of adjacent molecules, which leads to gelation at lower temperature.[50] A similar effect was previously reported by El-Enin and Gina[51] for the combination of hydroxypropyl methylcellulose and pluronic in the evaluation of tenoxicam liquid suppository.

Gelation Time

Ideally, the system is expected to gel immediately or within a brief time upon exposure to its gelation temperature to prevent its quick removal by mucociliary clearance. From Table 2, it is noticeable that increasing the concentration of either PF-127 or Na-alg decreased the gelation time. This result indicates that, the reduction of effective sol-gel transition temperature, which is associated with higher polymer concentration, is accompanied by shorter gelation time.[52]

Viscosity and Rheological Behavior

From the results listed in Table 2, the viscosities of *in situ* gel formulae increased greater than 10 times when temperature was increased from 4°C to 37°C, which verifies the transition of the formulations from sol to gel at 37°C. It was also observed that increasing the concentration of PF-127 from 15% to 17% showed a slight increase in viscosity. This result indicates that the gel acquires greater entanglement and rigidity at higher PF-127 concentrations. El-Kamel[53] stated that, when the polymer concentration increases, the size and number of micelles within the gel structure increase. As a consequence, the intermicellar distance becomes shorter leading to a greater number of cross-links between neighboring micelles, which results in a higher viscosity.

Moreover, increasing the concentration of Na-alg from 0.25% to 0.75%, while keeping the pluronic concentration constant, increased also the viscosity of the preparations significantly (p <0.05). A study conducted by Lin et al.[54] investigated an *in situ* gelling system of pluronic/alginate mixture and observed that the combination of both polymers revealed higher viscosities than each polymer alone at physiologic conditions. Kulicke and Nottelmann[55] reported that water molecules may act as a cross-linking agent to form hydrogen bonds between the carboxyl groups of alginate and ether groups of pluronic, which may lead to the formation of a 3-dimensional network and stronger gel. Accordingly, under physiological conditions, the ionic repulsion between the negatively charged carboxyl groups may produce a more stretched alginate structure and thus form increased hydrogen bonds with the exposed PEO structure.[56] This indicates that combining Na-alg and pluronic under physiological conditions results in an *in situ* gelling system of greater gel strength.

Furthermore, when viscosity was measured in the presence of SNF, to explore the ion sensitive *in situ* gelling property of Na-alg, the *in situ* gel formulae showed greater viscosity values. It was reported by Zhang et al.[57] that alginate forms stable hydrogels in the presence of Ca^{2+} present in the nasal fluid at low concentrations through the ionic interaction between the cation and the carboxyl functional group of guluronic acid residues located on the polymer chain. The divalent cations bridge the negatively charged guluronic acid residues on the alginate polymer chain and form an egg-box structure.[58] However, despite the obvious increase in viscosity, the effect of alginate was not a synergistic one. This suggests that the concentration of Ca^{2+} (5 mM) in the SNF is not high enough for the applied alginate concentrations to form a strong gel.

The flow behavior of *in situ* gels not only influences their residence time on the administration site but also affects the spreadability on the mucosal tissue after application into the nasal cavity. Rheological evaluation revealed that the viscosity of the systems fell on the influence of shear stress, indicating that these *in situ* gels serve as a non-Newtonian pseudoplastic fluid with a typical shear thinning characteristic.

From the previous results, it could be concluded that, upon introducing the *in situ* gel formula into the nasal cavity, the system exhibits an increase in viscosity due to gelation, thus prolonging the nasal residence time; at the same time, due to the shear action resulting from the nasal mucociliary swing, the viscosity of the gel decreases, and the system more easily arrive at the upper nasal mucosa regions, which are critical for its brain delivery via the olfactory and trigeminal regions of the upper nasal mucosa.

Measurement of Mucoadhesive Force

Mucoadhesive force is an important physicochemical parameter for *in situ* gelling nasal preparations because it prevents the formulation from rapid drainage due to mucociliary clearance, and it prolongs its residence time at the site of application, thus decreases the frequency of administration. The strength of mucoadhesion between polymer chains and the glycoprotein chains attached to the epithelial cells of mucus membranes depends on many factors, including amount, type and molecular weight of polymer, length of polymer chain, degree of hydration, degree of interpenetration of polymer chains in addition to type of bonding between polymer chains and mucosal surface.[59] The bonding of mucoadhesive polymers to mucosal membrane occurs primarily through hydrophobic interactions, hydrogen bonding, van der Waals bonds, and ionic interactions.[60]

The results, listed in Table 2, reveal that increasing the PF-127 concentration did not greatly affect the mucoadhesive strength of the *in situ* gels, but increasing the concentration of Na-alg significantly enhanced their mucoadhesive property (p <0.05).

Na-alg is known to swell rapidly, which facilitates the formation of an adhesive interaction between alginate and mucosa and contributes to the establishment of a more extensive cohesive layer, resulting in superior levels of mucosal retention.[61] The mucoadhesive force of alginate is probably because of the presence of hydroxyl groups on the polymer chain, which could form hydrogen bonds with mucin in addition to the anionic nature of the polymer, which promotes its mucoadhesion. It has been reported that polyanion polymers are more effective bioadhesive than polycation polymers or nonionic polymers.[62] Moreover, the increase in polymer concentration, which results in a longer penetrating chain length, was accompanied by an increase in bioadhesion.

The physicochemical characterization of all *in situ* gelling formulae revealed that G3, which showed the highest viscosity and mucoadhesion at an acceptable transition temperature, was selected as a carrier for nanolipid particles for *in vivo* study.

*Anticonvulsant Action Evaluation (*In Vivo *Study)*

For this study, the optimized CZ-loaded NLC formula (F5) was incorporated in the *in situ* gel showing the most satisfactory physicochemical properties (G3) and applied to the nostrils of the mice of Gp I. Furthermore, to test the effect of superparamagnetic iron oxide in improving the targeting of nanolipid carriers to brain by applying an external electrical field, F5S formula that incorporates SPION nanoparticles was incorporated also in G3 and applied intranasally to the mice of Gp II. The anticonvulsant action was evaluated by means of determining the onset time of the first clonic convulsion and time of death for Gp I and Gp II in

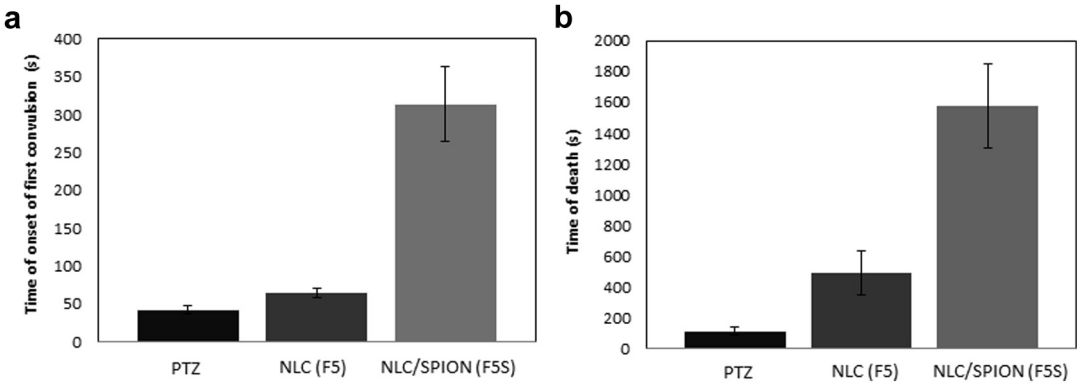

Figure 3. (a) Onset of first convulsion (s) and (b) time of death (s) of Swiss Albino mice with chemically induced convulsions when treated with CZ-loaded NLC (F5) incorporated in thermosensitive mucoadhesive *in situ* gel (G3) (Gp I, $n = 10$) and CZ-loaded NLC/SPION (F5S) incorporated in thermosensitive mucoadhesive *in situ* gel (G3) (Gp II, $n = 10$) in comparison to control group that did not receive any medication (Gp III, $n = 10$).

comparison to the control group (Gp III) that received no medication.

The results showed that the administration of pentylenetetrazole to sham-operated animals (Gp III) induced clonic convulsions with mean onset time of 41.7 ± 5.6 s that ended in death of the animals with mean death time of 113.5 ± 24.6 s ($n = 10$). Treatment of Swiss Albino mice with CZ-loaded NLC *in situ* gel (Gp I) in a dose of 0.2 mg/kg mouse, significantly prolonged the onset time for convulsion about 1.5 times (64.9 ± 6.3 s) and prolonged the onset time of death about 5 times (552.6 ± 102.3 s). Interestingly, the incorporation of SPION to the NLC (Gp II) delayed the onset time for first convulsion about 7.5 times (313.6 ± 49.5 s), and delayed the time of death up to 14 times (1574.6 ± 272.8 s) in comparison to the control group (Fig. 3).

Intranasal administration of nanoparticles has potential advantages in brain drug delivery especially nanolipid particles present an ideal delivery system for drugs through nasal tissue, which acts like most other biological membranes as a "lipid sieve". Nanoparticles can reach the brain by different mechanisms. The first mechanism involves passing of nanoparticles across epithelia and access to the blood stream directly via endocytosis or via lymphatic pathways, resulting in systemic distribution of nanoparticles, which then pass through the BBB. However, once nanoparticles are translocated into the blood stream, they could induce adverse biological effects or suffer from rapid clearance by reticuloendothelial system. The olfactory region, however, plays the most important part in the transportation of drugs to the central nervous system. Human olfactory mucosa, located on the roof of the nasal cavity, contains olfactory cells, which are bipolar neurons with one pole in contact with the external environment and another pole in the olfactory nerves, which enter the olfactory bulbs.[63] Nanoparticles, when applied deeply into the nasal cavity, can reach the brain by getting along axons of the olfactory nerve to the olfactorius and encephalic region, and then be distributed to the central nervous system.[64] Betbeder et al.[65] reported that morphine encapsulated in polysaccharidic nanoparticles showed significantly greater mice brain availability and antinociceptive effect upon nasal mucous administration than that of a common morphine preparation.

However, the epithelium of the nasal passage is covered by a mucus blanket, which entraps particles to be cleared from the nasal cavity and renewed by cilia. The nasal mucous cilia play a defensive role in maintaining the normal physiological environment of the nasal cavity and in the meantime are capable of clearing the drug or preparation particles together. To promote drug transport to the brain, the clearance effect of nasal mucous membrane cilia should be weaken by prolonging the contact time of the drug at tissues, especially to increase the deposition of drug on the olfactory mucosa.[66] In the present study, a longer retention could be satisfactory, achieved by incorporating the nanoparticles in a thermosensitive mucoadhesive *in situ* gel. The enclosure of SPION also enhanced significantly ($p < 0.01$) the brain targeting as revealed by the results. Through an external magnetic field, the nanoparticles could be satisfactory directed to the target tissue.

Conclusion

In the present study, CZ-loaded SPION/NLC incorporated in a pluronic PF-127–based thermosensitive mucoadhesive *in situ* gel efficiently targeted the drug to the brain via olfactory route and considerably protected the animals against chemically induced convulsions. The formulation provided on one hand an easy application because of its liquid nature when administered, and on the other hand, a better and longer retention at application site through its thermosensitive gelling and mucoadhesive properties. Furthermore, the nanoparticles could be guided more efficiently to the olfactory nerve endings by applying an external magnetic field. The developed formulation presents a very promising dosage form to deliver the drug directly to the brain in smaller doses with a consequent reduction in peripheral side effects.

Acknowledgments

The authors are grateful to Prof. Dr. Ebeid El-Zeiny, Tanta University, Egypt for his help with the synthesis of SPION.

All research data used in the preparation of the work is brought up in the manuscript.

References

1. Hirtz D, Thurman DJ, Gwinn-Hardy K, Mohamed M, Chaudhuri AR, Zalutsky R. How common are the "common" neurologic disorders? *Neurology*. 2007;68:326-337.
2. Chouinard G, Young SN, Annable L. Antimanic effect of clonazepam. *Biol Psychiatry*. 1983;18:451-466.
3. Steentoft A, Linnet K. Blood concentrations of clonazepam and 7-aminoclonazepam in forensic cases in Denmark for the period 2002–2007. *Forensic Sci Int*. 2009;184:74-79.
4. Alvarez N, Besag F, Iivanainen M. Use of antiepileptic drugs in the treatment of epilepsy in people with intellectual disability. *J Intellect Disabil Res*. 1998;42 Suppl 1:1-15.
5. Amidon GL, Lennernäs H, Shah VP, Crison JR. A theoretical basis for a biopharmaceutic drug classification: the correlation of *in vitro* drug product dissolution and *in vivo* bioavailability. *Pharm Res*. 1995;12:413-420.

6. Puglia C, Bonina F, Trapani G, Franco M, Ricci M. Evaluation of *in vitro* percutaneous absorption of lorazepam and clonazepam from hydro-alcoholic gel formulations. *Int J Pharm*. 2001;228:79-87.
7. Vyas TK, Babber AK, Sharma RK, Singh S, Misra A. Intranasal mucoadhesive microemulsions of clonazepam: preliminary studies on brain targeting. *J Pharm Sci*. 2006;95:570-580.
8. Shaji J, Poddar A, Iyer S. Brain-targeted nasal clonazepam microspheres. *Indian J Pharm Sci*. 2009;71:715.
9. Nour SA, Abdelmalak NS, Naguib MJ, Rashed HM, Ibrahim AB. Intranasal brain-targeted clonazepam polymeric micelles for immediate control of status epilepticus: *in vitro* optimization, *ex vivo* determination of cytotoxicity, *in vivo* biodistribution and pharmacodynamics studies. *Drug Deliv*. 2016;23:3681-3695.
10. Nour SA, Abdelmalak NS, Naguib MJ. Transferosomes for trans-nasal brain delivery of clonazepam: preparation, optimization, *ex-vivo* cytotoxicity and pharmacodynamic study. *J Pharm Res*. 2017;1(2):1-15.
11. Leyva-Gómez G, González-Trujano ME, López-Ruiz E, et al. Nanoparticle formulation improves the anticonvulsant effect of clonazepam on the pentylenetetrazole-induced seizures: behavior and electroencephalogram. *J Pharm Sci*. 2014;103:2509-2519.
12. Patel S, Chavhan S, Soni H, et al. Brain targeting of risperidone-loaded solid lipid nanoparticles by intranasal route. *J Drug Target*. 2011;19:468-474.
13. Yasir M, Sara UVS. Solid lipid nanoparticles for nose to brain delivery of haloperidol: *in vitro* drug release and pharmacokinetics evaluation. *Acta Pharm Sin B*. 2014;4:454-463.
14. Soane RJ, Frier M, Perkins AC, Jones NS, Davis SS, Illum L. Evaluation of the clearance characteristics of bioadhesive systems in humans. *Int J Pharm*. 1999;178:55-65.
15. Robinson JR, Mlynek GM. Bioadhesive and phase-change polymers for ocular drug delivery. *Adv Drug Deliv Rev*. 1995;16:45-50.
16. Krauland AH, Leitner VM, Bernkop-Schnürch A. Improvement in the *in situ* gelling properties of deacetylated gellan gum by the immobilization of thiol groups. *J Pharm Sci*. 2003;92:1234-1241.
17. Butoescu N, Jordan O, Burdet P, et al. Dexamethasone-containing biodegradable superparamagnetic microparticles for intra-articular administration: physicochemical and magnetic properties, *in vitro* and *in vivo* drug release. *Eur J Pharm Biopharm*. 2009;72:529-538.
18. Mahmoudi M, Sant S, Wang B, Laurent S, Sen T. Superparamagnetic iron oxide nanoparticles (SPIONs): development, surface modification and applications in chemotherapy. *Adv Drug Deliv Rev*. 2011;63:24-46.
19. El-Laithy HM, Nesseem DI, Shoukry M. Evaluation of two *in situ* gelling systems for ocular delivery of Moxifloxacin: *in vitro* and *in vivo* studies. *J Chem Pharm Res*. 2011;3:66-79.
20. Higuchi T. Mechanism of sustained-action medication. Theoretical analysis of rate of release of solid drugs dispersed in solid matrices. *J Pharm Sci*. 1963;52:1145-1149.
21. Asasutjarit R, Thanasanchokpibull S, Fuongfuchat A, Veeranondha S. Optimization and evaluation of thermoresponsive diclofenac sodium ophthalmic *in situ* gels. *Int J Pharm*. 2011;411:128-135.
22. Qi H, Chen W, Huanga C, et al. Development of a poloxamer analogs/carbopol-based *in situ* gelling and mucoadhesive ophthalmic delivery system for puerarin. *Int J Pharm*. 2007;337(1):178-187.
23. Sultana Y, Aqil M, Ali A, Zafar S. Evaluation of carbopol-methyl cellulose based sustained-release ocular delivery system for pefloxacin mesylate using rabbit eye model. *Pharm Dev Technol*. 2006;11:313-319.
24. Samia O, Hanan R, Kamal el T. Carbamazepine mucoadhesive nanoemulgel (MNEG) as brain targeting delivery system via the olfactory mucosa. *Drug Deliv*. 2012;19(1):58-67.
25. Gowda D, Tanuja D, Khan M, Desai J, Shivakumar H. Formulation and evaluation of *in situ* gel of diltiazem hydrochloride for nasal delivery. *Der Pharmacia Lettre*. 2011;3:371-381.
26. Banziger R, Hane D. Evaluation of a new convulsant for anticonvulsant screening. *Arch Int Pharmacodyn Ther*. 1967;167:245.
27. Abdel-Bar HM, Abdel-Reheem AY, Awad GAS, Mortada ND. Evaluation of brain targeting and mucosal integrity of nasally administrated nanostructured carriers of a CNS active drug, clonazepam. *J Pharm Pharm Sci*. 2013;16:456-469.
28. Westesen K, Siekmann B, Koch MHJ. Investigations on the physical state of lipid nanoparticles by synchrotron radiation X-ray diffraction. *Int J Pharm*. 1993;93:189-199.
29. Swidan SA, Ghonaim HM, Samy AM, Ghorab MM. Comparative study of solid lipid nanoparticles and nanostructured lipid carriers for *in vitro* Paclitaxel delivery. *J Chem Pharm Res*. 2016;8:482-493.
30. Honary S, Zahi F. Effect of zeta potential on the properties of nano-drug delivery systems - a review (part 1). *Trop J Pharm Res*. 2013;12:255-264.
31. Hornig S, Bunjes H, Heinze T. Preparation and characterization of nanoparticles based on dextran–drug conjugates. *J Colloid Interface Sci*. 2009;338:56-62.
32. Han F, Li S, Yin R, Liu H, Xu L. Effect of surfactants on the formation and characterization of a new type of colloidal drug delivery system: nanostructured lipid carriers. *Colloids Surf A Physicochem Eng Asp*. 2008;315:210-216.
33. López-García R, Ganem-Rondero A. Solid lipid nanoparticles (SLN) and nanostructured lipid carriers (NLC): occlusive effect and penetration enhancement ability. *J Cosmet Dermatol Sci Appl*. 2015;5:62.
34. Chinsriwongkul A, Chareanputtakhun P, Ngawhirunpat T, et al. Nanostructured lipid carriers (NLC) for parenteral delivery of an anticancer drug. *AAPS PharmSciTech*. 2012;13:150-158.
35. Kelidar HR, Saeedi M, Akbari J, et al. Development and optimisation of spironolactone nanoparticles for enhanced dissolution rates and stability. *AAPS PharmSciTech*. 2017;18:1469-1474.
36. Shafie M, Fayek H. Formulation and evaluation of betamethasone sodium phosphate loaded nanoparticles for ophthalmic delivery. *J Clin Exp Ophthalmol*. 2013;4(2):1-11.
37. Souto EB, Wissing SA, Barbosa CM, Müller RH. Development of a controlled release formulation based on SLN and NLC for topical clotrimazole delivery. *Int J Pharm*. 2004;278:71-77.
38. Aburahma MH, Badr-Eldin SM. Compritol 888 ATO: a multifunctional lipid excipient in drug delivery systems and nanopharmaceuticals. *Expert Opin Drug Deliv*. 2014;11:1865-1883.
39. Priyanka K, Sathali AA. Preparation and evaluation of montelukast sodium loaded solid lipid nanoparticles. *J Young Pharm*. 2012;4(3):129-137.
40. Khan S, Baboota S, Ali J, Narang RS, Narang JK. Chlorogenic acid stabilized nanostructured lipid carriers (NLC) of atorvastatin: formulation, design and *in vivo* evaluation. *Drug Dev Ind Pharm*. 2016;42:209-220.
41. McBain SC, Yiu HHP, Dobson J. Magnetic nanoparticles for gene and drug delivery. *Int J Nanomedicine*. 2008;3:169.
42. Prabha S, Zhou W-Z, Panyam J, Labhasetwar V. Size-dependency of nanoparticle-mediated gene transfection: studies with fractionated nanoparticles. *Int J Pharm*. 2002;244:105-115.
43. Dumortier G, Grossiord JL, Agnely F, Chaumeil JC. A review of poloxamer 407 pharmaceutical and pharmacological characteristics. *Pharm Res*. 2006;23:2709-2728.
44. Arora P, Sharma S, Garg S. Permeability issues in nasal drug delivery. *Drug Discov Today*. 2002;7:967-975.
45. Rao M, Agrawal DK, Shirsath C. Thermoreversible mucoadhesive *in situ* nasal gel for treatment of Parkinson's disease. *Drug Dev Ind Pharm*. 2017;43(1):142-150.
46. Soliman GM, Fetih G, Abbas AM. Thermosensitive bioadhesive gels for the vaginal delivery of sildenafil citrate: *in vitro* characterization and clinical evaluation in women using clomiphene citrate for induction of ovulation. *Drug Dev Ind Pharm*. 2017;43:399-408.
47. Rajoria G, Gupta A. In-situ gelling system: a novel approach for ocular drug delivery. *Am J PharmTech Res*. 2012;2:25-53.
48. Wanka G, Hoffmann H, Ulbricht W. Phase diagrams and aggregation behavior of poly(oxyethylene)-poly(oxypropylene)-poly(oxyethylene) triblock copolymers in aqueous solutions. *Macromolecules*. 1994;27:4145-4159.
49. Bhandwalkar MJ, Avachat AM. Thermoreversible nasal *in situ* gel of venlafaxine hydrochloride: formulation, characterization, and pharmacodynamic evaluation. *AAPS PharmSciTech*. 2013;14:101-110.
50. El Hady SA, Mortada ND, Awad GA, Zaki NM, Taha RA. Development of *in situ* gelling and mucoadhesive mebeverine hydrochloride solution for rectal administration. *Saudi Pharm J*. 2003;11:159-171.
51. El-Enin ASA, Gina S. Formulation and evaluation of in-situ gelling tenoxicam liquid suppositorie. *J Med Life*. 2013;1:23-32.
52. Ricci E, Lunardi L, Nanclares D, Marchetti J. Sustained release of lidocaine from poloxamer 407 gels. *Int J Pharm*. 2005;288:235-244.
53. El-Kamel AH. *In vitro* and *in vivo* evaluation of Pluronic F127-based ocular delivery system for timolol maleate. *Int J Pharm*. 2002;241:47-55.
54. Lin H-R, Sung KC, Vong W-J. *In situ* gelling of alginate/pluronic solutions for ophthalmic delivery of pilocarpine. *Biomacromolecules*. 2004;5:2358-2365.
55. Kulicke WM, Nottelmann H. Polymers in aqueous media: performance through association. In: Glass JE, ed. *Advances in Chemistry Series*. Washington, DC: American Chemical Society; 1989:15-44.
56. Lin H-R, Sung KC. Carbopol/pluronic phase change solutions for ophthalmic drug delivery. *J Control Release*. 2000;69:379-388.
57. Zhang P, Liu Z, Feng N, Xu J. Preparation and evaluation of self-microemulsifying drug delivery system of oridonin. *Int J Pharm*. 2008;355:269-276.
58. Grant GT, Morris ER, Rees DA, Smith PJC, Thom D. Biological interactions between polysaccharides and divalent cations: the egg-box model. *FEBS Lett*. 1973;32:195-198.
59. Andrews GP, Laverty TP, Jones DS. Mucoadhesive polymeric platforms for controlled drug delivery. *Eur J Pharm Biopharm*. 2009;71:505-518.
60. Woodley J. Bioadhesion. *Clin Pharmacokinet*. 2001;40:77-84.
61. Richardson JC, Dettmar PW, Hampson FC, Melia CD. Oesophageal bioadhesion of sodium alginate suspensions: 2. Suspension behaviour on oesophageal mucosa. *Eur J Pharm Sci*. 2005;24:107-114.
62. Sachan NK, Pushkar S, Jha A, Bhattcharya A. Sodium alginate: the wonder polymer for controlled drug delivery. *J Pharm Res*. 2009;2:1191-1199.
63. Thorne RG, Frey 2nd WH. Delivery of neurotrophic factors to the central nervous system: pharmacokinetic considerations. *Clin Pharmacokinet*. 2001;40:907-946.
64. Oberdörster G, Sharp Z, Atudorei V, et al. Translocation of inhaled ultrafine particles to the brain. *Inhal Toxicol*. 2004;16:437-445.
65. Betbeder D, Spérandio S, Latapie J-P, et al. Biovector™ nanoparticles improve antinociceptive efficacy of nasal morphine. *Pharm Res*. 2000;17:743-748.
66. Charlton ST, Davis SS, Illum L. Evaluation of bioadhesive polymers as delivery systems for nose to brain delivery: *in vitro* characterisation studies. *J Control Release*. 2007;118:225-234.